Generation of Ultraintense Proton Beams Driven by a Short-Pulse Multi-TW Laser

J. Badziak, [1*] S. Jabłoński,[1] P. Parys,[1] M. Rosiński,[1] J. Wołowski,[1] A. Szydłowski,[2] P. Antici,[3] J. Fuchs,[3] A. Mancic[3]

[1]*Institute of Plasma Physics and Laser Microfusion, EURATOM Association, 00-908 Warsaw, Poland*
[2]*Andrzej Soltan Institute for Nuclear Studies, Świerk, Poland*
[3]*LULI, Ecole Polytechnique, CNRS, CEA, UPMC; Route de Saclay, 91128 Palaiseau, France*

Received January 5, 2009; accepted February 23, 2009; published March 31, 2009

Abstract— The results of experimental studies of high-intensity proton beam generation at the interaction of a 350 fs laser pulse of 1.06μm or 0.53μm wavelength and intensity up to 2×10^{19}Wcm^{-2} with a thin (0.6 -3μm) solid target are reported. It is shown that collimated MeV proton beams of intensity ~ 10^{18} Wcm^{-2} and current density ~ 10^{12}Acm^{-2} at the source can be produced when the laser-target interaction conditions approach the skin-layer ponderomotive acceleration requirements and the laser intensity-wavelength product is above 10^{19}Wcm^{-2}μm^2. The effect of laser intensity, the target structure and the laser wavelength on the proton beam intensity and the laser-protons energy conversion efficiency are demonstrated.

Recent progress in laser technology has resulted in the construction of short-pulse lasers producing picosecond or femtosecond pulses of power approaching 1PW (10^{15}W) and intensities exceeding 10^{20}W/cm^2 [1, 2]. The interaction of a laser pulse of such extreme parameters with a solid target can lead to the production of collimated ion beams of high ion energy (of MeV to GeV energies), of short time duration (down to subps) and of very high power (ion currents) and beam intensity (ion current densities) [2–4], unattainable with conventional accelerators. Such ion beams have the potential to be applied in various areas of science, technology and medicine. The possible ion beam applications can be roughly divided in two groups. The first one – which includes, for example, nuclear and particle physics [5, 6], hadron therapy of cancers [7] and proton radiography [3] – requires high ion energies (from tens to hundreds of MeV and beyond) and, possibly, a narrow ion energy spectrum, while ion beam power, P_i, and intensity, I_i , can be moderate. In the second group – which includes high energy-density physics [8, 9] and fast ignition (FI) of inertial fusion [10, 11] as well as ion implantation [12] or radioisotope production for positron emission tomography (PET) [13] – mean ion energies ≤ 10 MeV are sufficient but ion beam power and intensity should be very high (for instance, FI requires a proton beam of the mean proton energy E_p~3–5MeV, and $I_i \geq 5\times10^{19}$W/cm^2 [11]).

* E-mail: badziak@ifpilm.waw.pl

A recognized and successful laser method of producing collimated, high-ion-energy beams is target normal sheath acceleration (TNSA), e.g. [2–4, 14]. In this method, ions are accelerated at the rear surface of the foil target by a virtual cathode (Debye sheath) created by hot electrons produced by a laser pulse at the target front and penetrating through the target. It has been demonstrated that at relativistic laser intensity I_L (i.e. at $I_L\lambda^2 > 10^{18}$Wcm^{-2}μm^2, where λ is the laser wavelength) TNSA can produce collimated ion beams of maximum energy of tens of MeV for protons (e.g. [2–4, 15]) or of several MeV/amu for heavier ions [4, 16, 17]. However, the ion density of TNSA beams is relatively low (≤ 10^{19}cm^{-3}) and, as a result, the ion beam intensity $I_i = n_i\upsilon_i E_i$ or current density $j_i = zen_i\upsilon_i$ are usually moderate (z is ion charge state, e is the elementary charge, n_i, υ_i, E_i are ion density, velocity and energy, respectively). For producing high-intensity high-power ion beams for the second group of application, skin-layer ponderomotive acceleration (SLPA) [4, 18–21] seems to be a more promising method. In this method, the ponderomotive pressure induced by a short laser pulse near the critical plasma surface drives forward a dense plasma (ion) bunch of ion density (n_i) higher than the plasma critical density. As $n_i > 10^{21}$-10^{22} cm^{-3} [4, 20, 22], even at moderate ion velocity and energy, the intensity of SLPA-driven ion beams can be very high, much higher than in the case of TNSA beams. The SLPA beam intensity can still be increased by beam focusing, using the curved target front surface [23].

This paper reports the results of experimental studies of laser-driven generation of high-intensity proton beams performed on the LULI 100TW Nd:glass laser facility at Ecole Polytechnique (Palaiseau, France). The effect of laser intensity, target structure and laser wavelength on proton beam parameters and laser-protons energy conversion efficiency is demonstrated.

In the experiment, a 350-fs, 1ω or 2ω Nd:glass laser pulse of high contrast ratio (~ 10^7 for 1ω and > 10^8 for 2ω) and intensity up to 2×10^{19}W/cm^2 irradiated a thin (0.6 – 3μm) PS (polystyrene) or Au/PS (PS covered by

0.05 – 0.2μm Au front layer) target along the target normal. As the preplasma density gradient scale length near the critical surface, L_n, was relatively small ($L_n < 2$ – 3μm for 1ω [24] and $L_n < 1$μm for 2ω) and the laser beam diameter on the target, d_L, was ≈ 10–50μm, the condition $d_L >> L_n$, λ, L_T required for SLPA [4, 19, 20] was quite well fulfilled, especially for larger d_L and/or 2ω laser beam (L_T is the target thickness). The proton beam characteristics were measured using the time-of-flight method (four ion charge collectors [19, 25]), solid state track detectors (SSTDs) [26] and radiochromic films (RCFs) [3].

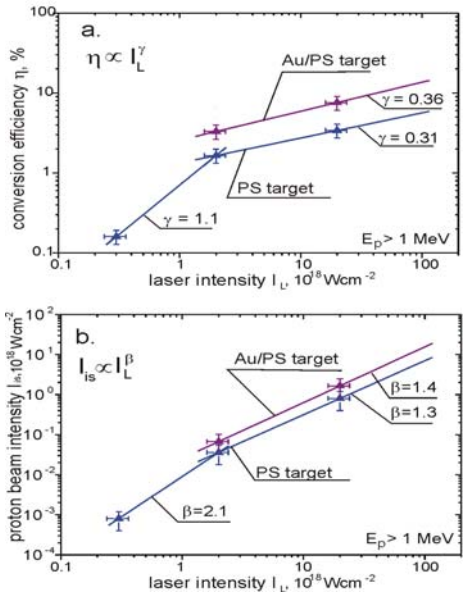

Fig. 1. Laser-protons energy conversion efficiency and proton beam intensity at the source as a function of laser intensity for PS and Au/PS targets. Points represent the results of IC measurements, lines – the results of approximation by a power function.

The dependences of laser-protons energy conversion efficiency (η) and intensity at the source of the proton beam generated from 1.8-μm PS target and Au/PS target with 0.2-μm Au layer on the laser intensity, for protons of energies 1MeV < E_p < 3 MeV, are presented in Fig.1. The proton beam intensity at the source was calculated from the IC measurements using the formula [4, 19]: $I_{is} \approx \overline{E}_p Q/e\tau_s S_s$, where Q is the total charge of protons of mean energy $\overline{E}_p$ (in the considered energy range), τ_s is the proton pulse duration at the source, S_s is the proton beam area at the source and e is the elementary charge. As for SLPA ions τ_s is approximately equal to the laser pulse duration τ_L and S_s is close to the laser focal spot area $S_L = \pi d_L^2$ [4, 19 – 21, 27], so to calculate I_{is} we assumed $\tau_s \approx \tau_L$, $S_s \approx S_L$. It can be seen that for moderate-energy protons the conversion efficiency and the proton beam intensity for the Au/PS target is twice as high as for the PS target and they approach 8% and 2×10^{18}W/cm^2, respectively, at $I_L = 2\times10^{19}$W/cm^2 (the indicated value of I_{is} corresponds to the value of proton current density $j_{is} = zeI_{is}/\overline{E}_p \approx 10^{12}$A/cm^2). A similar increase in η and I_{is} for the Au/PS target was also observed for high-energy protons (>3MeV).

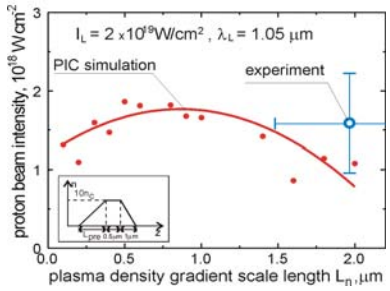

Fig. 2. Proton beam intensity at the source as a function of the preplasma density gradient scale length. Solid line – an approximation of the results of PIC simulations (points). Open circle with error bars – the result of measurements.

We compared the proton beam intensity obtained from the measurements with the results of particle-in-cell (PIC) numerical simulations using a fully electromagnetic, relativistic 1D (one-dimensional) PIC code. In the case presented in Fig. 2, a 0.35-ps, a 1-μm laser pulse of quasi-Gaussian time shape (∝ exp [-t^4]) and the peak intensity of 2×10^{19}W/cm^2 interacted with an inhomogeneous, fully ionized hydrogen plasma layer of the density profile shown in the frame inside of the figure. It can be seen that the proton beam intensity is a non-monotonic function of the preplasma density gradient scale length $L_n = n_{ec}^o \left(\partial n_e / \partial z\right)_{z=z_c}^{-1}$ with a maximum (above 10^{18}W/cm^2) at $L_n \approx 0.8$ μm. The experimental value of I_{is} agrees quite well (within factor 2) with that from the simulations.

To reach a relatively high laser pulse contrast ratio needed for effective SLPA proton generation, a 2ω (second harmonic) laser beam for proton generation can be used as an alternative to the commonly employed 1ω beam proton driver. A comparison of measurements of proton beam parameters performed for 1ω and 2ω beam of the LULI 100TW laser is presented in Fig.3. When $I_L\lambda^2$ for the 1ω beam is equal to that for the 2ω beam, the beam intensity of protons of energy 1 – 3MeV (Fig. 3a) is nearly 10 times higher and conversion efficiency is about 40% higher for the 2ω beam than that for the 1ω beam, in spite of the fact that the 2ω laser beam energy was more than twice as low. Also, the number (per cm^2) of high-energy (> 3 MeV) protons is higher for 2ω (Fig. 3b). However, for $I_L^{1\omega} \approx I_L^{2\omega}$, the beam intensity of 1-3MeV protons is comparable for 1ω

and 2ω and the laser-protons conversion efficiency is lower for the 2ω

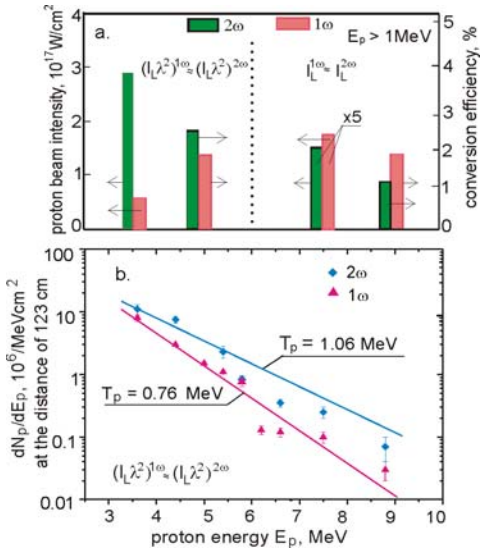

Fig. 3. A comparison of parameters of moderate-energy (1 – 3MeV) (a) and high-energy (>3MeV) (b) proton beams generated by a 1ω or 2ω laser beam. $I_L^{1\omega} \approx 2\times10^{18}$W/cm^2. For part (b): points – the results of SSTD measurements, lines – the results of approximation by the Maxwellian energy distribution with temperature T_p.

beam. These results are in fairly good agreement with our PIC simulations in which we observed that for the case $\left(I_L\lambda^2\right)^{1\omega} = \left(I_L\lambda^2\right)^{2\omega}$ the beam intensity of protons generated by a 2ω beam was 3 – 10 times higher (depending on L_n) than that for a 1ω beam.

The angular divergence (Θ_p) of proton beams driven by both the 1ω beam and the 2ω beam was rather small and for relativistic laser intensities, typically, Θ_p (1ω) ≈ 25° – 30° and Θ_p (2ω) ≈ 20° – 25° (Θ_p is the full angle cone at half maximum of the beam intensity). However, spatial (transverse) proton beam structures were different for the two considered cases. In the 1ω case we observed a ring-like spatial structure for both moderate-energy and high-energy protons. In the 2ω case, the beam structure was more homogeneous and for moderate-energy protons the maximum intensity was recorded close to the beam axis.

In conclusion, it has been shown that 1-3MeV proton beams of intensity ~ 10^{18}W/cm^2 and current density ~ 10^{12}A/cm^2 at the source can be produced at relativistic laser intensity (>10^{19}Wcm^{-2}μm^2) when the laser-target interaction conditions approach the SLPA requirements. The laser-protons energy conversion efficiency and proton beam parameters remarkably depend on the target structure and can be significantly increased with the use of a double-layer Au/PS target. The intensity of a proton beam generated by the 2ω laser beam is at least several times higher than that produced by the 1ω beam with the same value of $I_L\lambda^2$, while intensity is comparable when $I_L^{2\omega} \approx I_L^{1\omega}$. The values of proton beam intensity and current density attained in our experiment are the highest among the ones measured so far. It is believed that by an increase in the intensity and/or duration of a laser pulse driving protons as well as by careful optimization of the target structure they can be increased further, up to the values required for fast ignition of a fusion target.

The authors acknowledge the LULI laser team for their expert support in this experiment. The access to the LULI 100TW laser facility has been supported by the European Commission under the *LASERLAB-Europe Integrated Infrastructure Initiative (contract No. RII3-CT-2003-506350)*. This work was also supported in part by the IAEA RCP project under Contract No. 13794 as well as the IPPLM contribution to the HiPER project.

References

[1] [G.Mourou and D.Umstadter, Sci.Am. **286**, 80 (2002).
[2] L.Robson, et al., Nature Phys. **3**, 58 (2007).
[3] M. Borghesi, et al., Fusion Sci. Technol. **49**, 412 (2006) and references therein.
[4] J. Badziak, Opto-Electron. Rev. **15**, 1 (2007) and references therein.
[5] K.W.D. Ledingham, P. McKenna and R. Singhal, Science **300**, 1107 (2003) and references therein.
[6] A. Maksimchuk, et al., Plasma Phys. Rep. **30**, 473 (2004).
[7] S.V. Bulanov, et al., Phys. Lett. A **299**, 240, 2002.
[8] M. Koenig, et al., Plasma Phys. Control. Fusion **47**, B441 (2005).
[9] P.K. Patel, et al., Phys. Rev. Lett. **91**, 125004 (2003).
[10] M. H. Key, et al., Fusion Sci. Technol. **49**, 440 (2006) and references therein.
[11] J. Badziak, S. Jabłoński and J. Wołowski, Plasma Phys. Control. Fusion **49**, B651 (2007) and references therein.
[12] F. P. Boody, et al., Laser Part. Beams **14**, 443 (1996).
[13] S. Fritzler, et al., Appl. Phys. Lett. **83**, 3039 (2003).
[14] S.C. Wilks, et al., Phys. Plasmas, **8**, 542 (2001).
[15] R.A. Snavely, et al., Phys. Rev. Lett. **85**, 2945 (2000).
[16] B.M. Hegelich, et al., Phys. Plasmas **12**, 056314 (2005).
[17] P. McKenna, et al., Plasma Phys. Control. Fusion **49** B223 (2007).
[18] J. Badziak, et al., Appl. Phys. Lett. **85**, 3041 (2004).
[19] J. Badziak, et al., Laser Part. Beams **23**, 401 (2005).
[20] J. Badziak, S. Jabłoński, and S. Głowacz, Appl. Phys. Lett. **89**, 061504 (2006).
[21] T. V. Liseykina and A. Macchi, Appl. Phys. Lett. **91**, 171702, (2007).
[22] J. Badziak, et al., Laser Part. Beams **24**, 249 (2006).
[23] J.Badziak and S.Jabłoński, Appl. Phys.Lett. **90**, 151503 (2007).
[24] J. Fuchs, et al., Phys. Plasmas **14** 053105 (2007).
[25] J. Badziak, et al., J. Phys. D: Appl. Phys. **34**, 1885 (2001).
[26] A. Szydłowski et al., Radiat. Meas. **34**, 325 (2001).
[27] H. Habara, et al., Phys. Plasmas **10,** 3712 (2003).

